Journal of Visualization, Vol. 12, No. 3 (2009) 203-215

Regular Paper

Study on Concurrent Measurements of Velocity and Density Distributions for High-Speed CO_2 Flow

Kim, Y. –J.*[1], Okamoto, K.*[2] and Ko, H. S.*[3]

*1 Department of Mechanical Design, Sungkyunkwan University, 300 ChunChun-Dong, JangAn-Gu, Suwon, KyungGi-Do 440-746, Korea.
*2 Department of Human and Engineered Environmental Studies, School of Frontier Sciences, The University of Tokyo, 5-1-5 Kashiwano-ha, Kashiwa, 277-8563, Japan.
*3 School of Mechanical Engineering, Sungkyunkwan University, 300 ChunChun-Dong, JangAn-Gu, Suwon, KyungGi-Do 440-746, Korea.
E-mail: hanseoko@skku.edu

Received 31 October 2008
Revised 23 March 2009

Abstract : Velocity and density distributions of a high-speed and initial CO_2 jet flow have been analyzed concurrently by a developed three-dimensional digital speckle tomography and a particle image velocimetry (PIV). Two high-speed cameras have been used for the tomography and one for the PIV since a shape of a nozzle for the jet flow is bilaterally symmetric and the starting flow is fast and unsteady. The speckle movements between no flow and CO_2 jet flow have been obtained by a cross-correlation tracking method so that those distances can be transferred to deflection angles of laser rays for density gradients. The three-dimensional density fields for the high-speed CO_2 jet flow have been reconstructed from the deflection angles by the real-time tomography method, and the two-dimensional velocity fields have been calculated by the PIV method concurrently and instantaneously.

Keywords : Flow Visualization, Digital Speckle System, Tomography, Particle Image Velocimetry (PIV), Carbon Dioxide (CO_2)

1. Introduction

Recently many researchers have measured various physical properties simultaneously by advanced flow visualization techniques. Especially, there have been some studies about simultaneous measurements of distributions of density and other properties. For instance, a turbulent jet diffusion flame has been investigated by TV holography, schlieren studies, and large eddy simulations (LES) (Mattson et al., 2004). Combination of novel experiments, such as TV holography, and LES computations of the same jet flame has been focused in their study. Carlsson et al have also developed combination of schlieren and pulsed TV holography to analyze a high-speed flame jet (Carlsson et al., 2006). A deflectometry technique has been developed for the schlieren method to measure an unsteady flame quantitatively (Wong and Agrawal, 2006). The schlieren technique has been modified for micro-scale visualization of supersonic flow through a micronozzle setup (Huang et al., 2007). Simultaneous measurement techniques for temperature and velocity fields of thermal liquid flows have also been developed using the laser-induced fluorescence combined with the particle image velocimetry (PIV) (Fujisawa et al., 2008).

In this study, three-dimensional density fields and two-dimensional velocity fields have been

reconstructed concurrently for the high-speed CO_2 flow with the interval of 1/15,000 second and 2/15,000 second, respectively. The velocity distributions have been analyzed by the particle image velocimetry (PIV) (Raffel et al., 1998) and the density distributions have been reconstructed using the digital speckle tomography (Ko et al., 2001).

The digital speckle tomography is a combined technique of a digital specklegram and a tomography. The density distribution can be measured by the digital specklegram using a refraction of a light beam. Although the interferometry shows relatively precise results for small density gradients (Vest, 1979), the digital speckle method which is one of the deflectometry methods, is suitable for steep regions of the density gradients since the speckle moves clearly and the fringe shifts of the interferometry are too big to observe for these conditions (Ko et al., 2002). Thus, the digital speckle method has been used for the mixed flow of CO_2 and air, which gives great density difference. Also, the experimental setup of the speckle method is relatively simple and fast compared with the interferometry.

The tomography reconstructs the cross-sectional image of an asymmetric flow nonintrusively from transmitted or refracted data collected by illuminating the flow from different angles of view. An algebraic reconstruction technique (ART) and a multiplicative algebraic reconstruction technique (MART) are the representative tomography methods (Verhoeven, 1993) to obtain density or temperature distributions.

The PIV technique measures a velocity distribution quantitatively by visualizing flow fields with small tracer particles and analyzing visualized digital images with different times for particle movements (Erkan et al., 2008). The PIV can measure whole two-dimensional or three-dimensional flow field without disturbing the flow.

2. Digital Speckle System

The laser speckles are shown as a very fine pattern of bright and dark spots by a ground glass that diffracts coherent light in a constructive and destructive way. The speckles are dislocated from their original locations by the deflection angle of the incident rays since the ray of light is bent from its original path by variation of the index of refraction in the field. The digital speckle system records the original speckle image and the dislocated speckle image separately using the CCD camera to measure the speckle movements like a particle tracking method of the particle image velocimetry (PIV). The speckle displacements of the CO_2 flow from the elliptical nozzle can be obtained by the cross-correlation method (Raffel et al., 1998). Because most of the speckles in this study move perpendicularly to the flow direction, rectangular interrogation areas have been used instead of square ones (Ko et al., 2001).

The beam deflection angle α can be obtained from a ray integral of the field density gradient normal to the direction of the incident laser beam with the Gladstone-Dale constant K (Partington, 1953):

$$\psi_{SP} \cong \alpha = K \int \frac{\partial \rho}{\partial s} dt \tag{1}$$

where ψ_{SP} is the projection of the digital speckle system, α is the deflection angle, ρ is the field density, s is perpendicular to, and t is parallel to the incident ray.

The deflection angle, α in Eq. (1) must be inverted to reconstruct the true density field by the speckle tomography (Fomin, 1998). Since the tomography methods (Gordon, 1974) update the density distributions by using the feedback information of the density itself instead of the density gradient, the ray deflection angle ψ_{SP} from the digital speckle system should be converted to the interferometric fringe shift ψ_{IF} which can be expressed as the integration of the density itself (Ko and Kihm, 1999) from the integration of the deflection angle along the perpendicular direction of the light ray s as follows:

$$\psi_{IF} = \frac{1}{\lambda}\int \psi_{SP}\, ds \tag{2}$$

Equation (2) implies that an integral of the ray deflection angle, ψ_{SP}, along s is equivalent to the interferometric fringe shift number ψ_{IF}.

The procedure of the reconstruction of the density distribution has been shown in Fig. 1. Two digital images with and without CO_2 flow have been captured and the speckle displacements have been calculated by the cross-correlation method. Since the resolution of the camera is reduced to capture the high-speed images, the number of data decreases and the error increases for the high-speed capture. In order to obtain more accurate results by increasing the number of data, the captured images have been magnified to 1024×1024 pixels from 256×256 pixels using the bi-cubic method for the interpolation. Although more information cannot be obtained by the magnification, the error can be reduced greatly for the cross-correlation after increasing the number of pixels for the interrogation window size by the bi-cubic interpolation method. Since the size of the interrogation window has been selected to be 64×64 pixels in the magnified image for the digital speckle tomography, clear data of the speckle displacements without noise have been obtained as shown in Fig. 1. The fringe shift data in number of fringes have been calculated by integrating the speckle displacement data using a developed integration method, and the density distribution has been reconstructed by the tomography method from the fringe shift data.

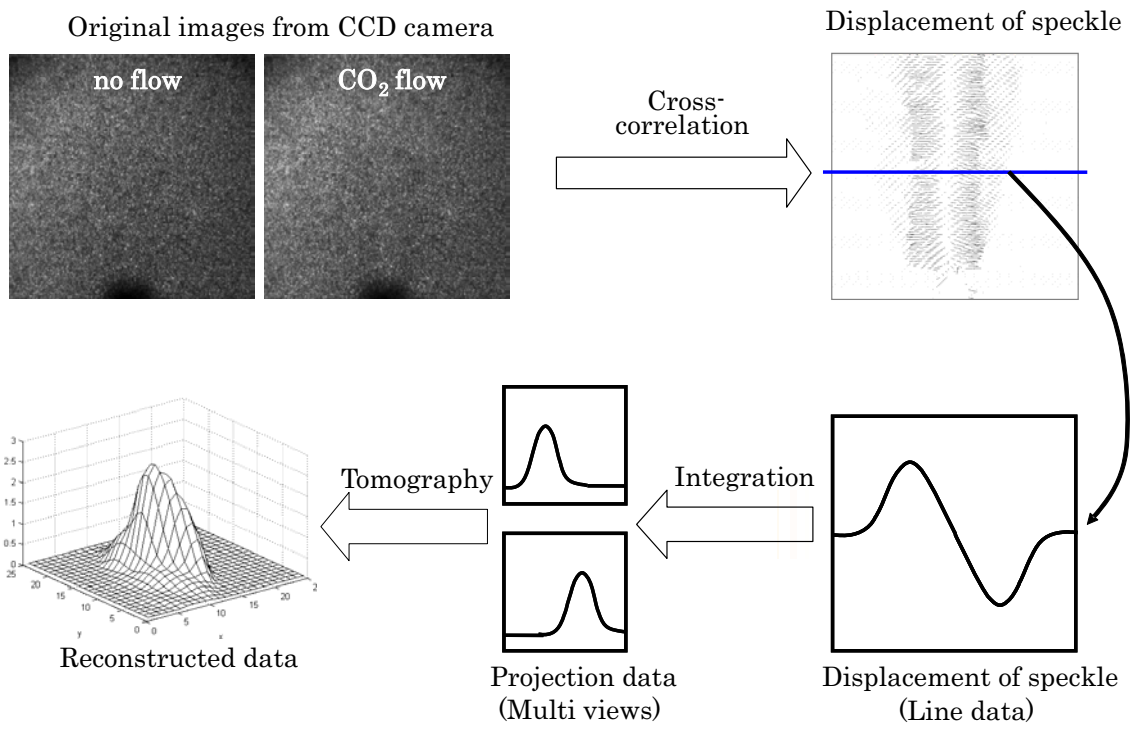

Fig. 1. Procedure of reconstruction of density distribution by digital speckle tomography.

The developed new integration method which is different from a conventional integration method has been used to calculate more accurate ψ_{IF} by modifying and integrating ψ_{SP}. The modification of ψ_{SP} is very important for this method to avoid inaccurate integration of discrete values. If the discrete values of ψ_{SP} are integrated without modification, ill-balanced results can be obtained between starting and ending points of the integration. Because the discrepancy of ψ_{IF} between those points is proportional to the total sum of ψ_{SP}, the numerical difference is subtracted

from the existing ψ_{SP} to obtain the balanced values. However, the shape of ψ_{IF} can be distorted if the average value of $\psi_{SP}$is subtracted evenly. Thus, the proportional value to the absolute ψ_{SP} has been subtracted from each original value of ψ_{SP} as follows:

$$\Psi'_{SP} = \Psi_{SP} - \sum_{i=1}^{n} \Psi_{SP}(i) \times \frac{|\Psi_{SP}|}{\sum_{i=1}^{n} |\Psi_{SP}(i)|} \tag{3}$$

where i denotes each discrete deflection angle in each projection angle of view and n denotes total number of deflection angles in each projection angle to calculate the fringe shift ψ_{IF}. The new ψ_{SP}' in Eq. (3) has been used to calculate ψ_{IF} in this study. The improvement of inequality for reasonable integration can be confirmed in Fig. 2. The developed integration method has been applied for reconstruction of the density distribution of CO_2 flow in this study.

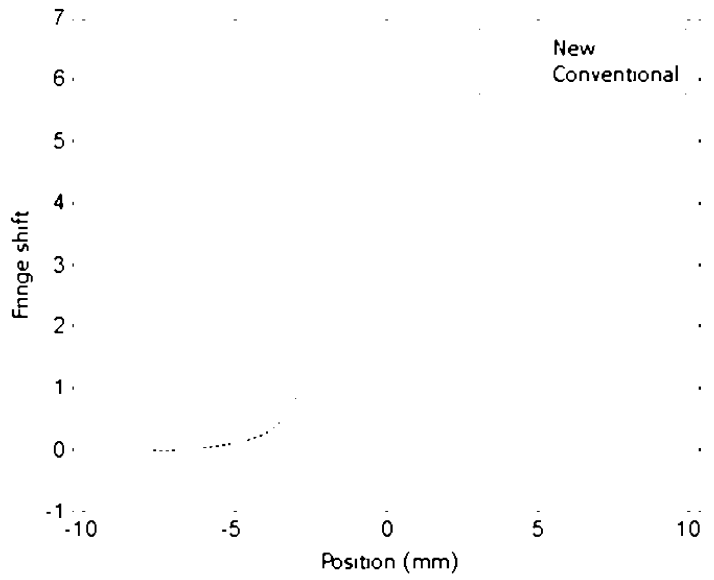

Fig. 2. Comparison between conventional and new integration method for projection data.

3. Tomographic Reconstruction Algorithm: Multiplicative Algebraic Reconstruction Technique (MART)

The true density field, $\rho(x,y,z)$ has been reconstructed from the deflection angle, α in Eq. (1) by the speckle tomography. Each basis function of the tomography is defined by a single parameter (its unknown height with a fixed spread) for the linear case. The location of each three-dimensional basis function is given as (Ko et al., 2006)

$$\hat{f}(x,y,z) = \sum_{j=1}^{JKL} O_j b(x - x_j, y - y_j, z - z_j) \tag{4}$$

where $\hat{f}$ is an object function that represents the field to be reconstructed, b is a general form of the basis function located at (x_j,y_j,z_j), and O_j is the height coefficient of the j-th basis function centered at a fixed location of (x_j,y_j,z_j). JKL means $J\times K\times L$ and a hexadral array of J, K and L equally spaced points in the x, y and z directions can be formed at the (x_j,y_j,z_j) positions, respectively. The deviations between the virtual projection $\hat{\psi}$ of an intermediate object function $\hat{f}$ and the measured projection ψ of the actual field f must be minimized in the optimized set of these unknowns.

The multiplicative algebraic reconstruction technique (MART) uses an element C_j of the multiplicative correction vector C as follows (Ko and Kihm, 1999; Verhoeven, 1993):

$$O_j^{q+1} = C_j^q O_j^q$$
$$C_j^q = \begin{cases} 1 - 0.5 W_{i,j}\left(1 - \dfrac{\psi_i}{\hat{\psi}_i}\right), & \hat{\psi}_i \neq 0 \\ 1, & \text{otherwise} \end{cases} \tag{5}$$

where i is the total number of ray sums, which is the number of ray sums for each projection angle times the number of projection angles in same plane times the number of planes in z direction (150×2×60 in this study), j is the total number of pixels in x, y and z directions (25×25×25 in this study) for the reconstructed field, q denotes the q-th iteration, and the normalized weighting factor $W_{i,j}$ is equal to $w_{i,j}/w_{max}$ where w_{max} is the largest element of the projection matrix W.

The accuracy of the tomography has been investigated before the experiment using a computer-synthesized phantom field. The projection data for the deflection angles ψ_{SP} of the density gradients have been calculated from the phantom and then the phase shifts ψ_{IF} have been obtained from Eqs. (2) and (3). Then, the algebraic reconstruction technique (ART) and the MART have been performed numerically to reconstruct the refractive indices and calculate the relative densities for confirmation of accuracies. The calculated results of the MART show better reconstructions than those of the ART by comparing with the computer-synthesized phantom field (Ko et al., 2004; Ko et al., 2006).

4. Experimental Setup

A CO_2 gas tank, an oil particle generator, a solenoid valve and the nozzle have been connected by a flexible tube. The oil particle generator has been designed and manufactured by the authors and uniform oil particles with 10μm have been generated. The solenoid valve with a safe working pressure of 2.5MPa is closed without electricity and it takes 10ms to open the valve fully. The working fluid, CO_2 has always been passed through the oil generator to mix the CO_2 with the oil particles. The velocity data for the starting flow has been obtained by flowing the CO_2 from the tank with the oil particles after opening the valve. The experiment has been performed at the surrounding air of 20°C. Thus, the densities of pure CO_2 and air have been measured to be 1.8kg/m^3 and 1.2kg/m^3, respectively. The measured maximum velocity was 130m/s, which was lower than the sonic velocities of CO_2 and air (265.8m/s and 340m/s, respectively).

Initially, the tube has been filled with the CO_2 and released after opening the solenoid valve which controls the CO_2 flow from the nozzle. The nozzle was placed on an optical table with optical instruments for the digital specklegram and the PIV as shown in Fig. 3. Three high-speed cameras, two lasers, and the solenoid valve have been connected to the synchronized system so that the whole system can be operated at the same time. Figure 4 shows the time table of synchronization for the system. Although the PIV images have been captured at every 1/15,000 sec, the velocity distribution has been obtained with the interval of 2/15,000 sec because consecutive two images are required for the cross-correlation of the PIV experiment. The high peaks at the first and second rows in Fig. 4 show pulses of the laser (frequency of 7.5 kHz with double pulse) and camera exposures for the PIV. The density distribution can be reconstructed at every 1/15,000 second since the speckle image including the CO_2 flow is compared with the reference image without the flow for the cross-correlation of the digital speckle tomography. The peaks at the last row in Fig. 4 show camera exposures for the captured images with the CO_2 flow at every 1/15,000 second.

A laser beam from a continuous wave 50mJ Nd:YAG laser with a wavelength of 532nm has been expanded by a 10× microscopic objective lens and directed at an optical lens. The speckles for measuring the density distributions have been formed by a ground glass between the objective and

the optical lens. The laser beam has been divided into two beams by a beam splitter and the beams pass through the nozzle and are projected onto the viewing screens (Fig. 3). The speckle patterns on the viewing screens have been captured by two high-speed cameras and converted into digital images. The other laser beam from a pulsed wave 50mJ Nd:YAG laser has been stretched and narrowed by two cylindrical lenses so that the formed laser sheet can be passed through the center of the nozzle for the PIV experiment.

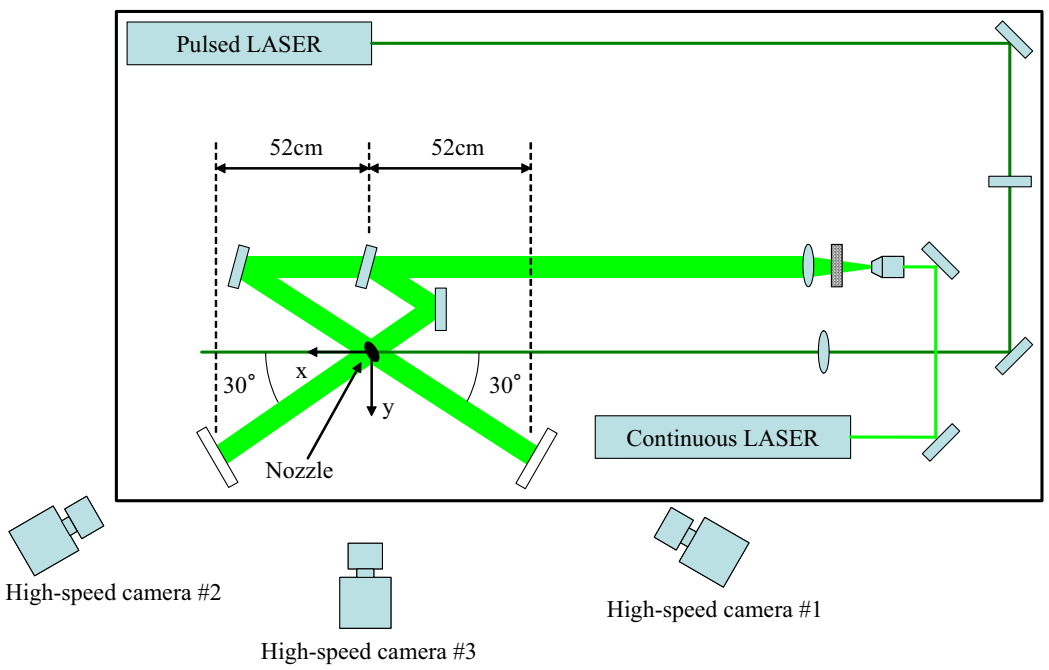

Fig. 3. Optical setting for digital speckle system and PIV.

Three high-speed cameras have been used to observe the starting flow of the CO_2 as shown in Fig. 3. Two high-speed cameras have been used for measurement of the three-dimensional density distribution of CO_2 flow from the nozzle and a third high-speed camera has been used for the two-dimensional velocity distribution. The angle between the first high-speed camera and the laser beam from the pulsed laser is 30 degree and the second one with 150 degree. The nozzle which has an elliptical shape with the width of 8mm and the height of 4mm was skewed about 120 degree from

x-axis (Fig. 3). The two high-speed cameras (Photron, APX) with 256×256 pixel resolution for the speckle method can capture 15,000 images at every second, and maximum 120,000 images per one second can be captured if the image size is reduced. The other high-speed camera (Photron, APX-RS) with 384×384 pixel resolution for the PIV has been fixed to be 15,000 captured images per one second and this camera can also capture maximum 250,000 images per one second.

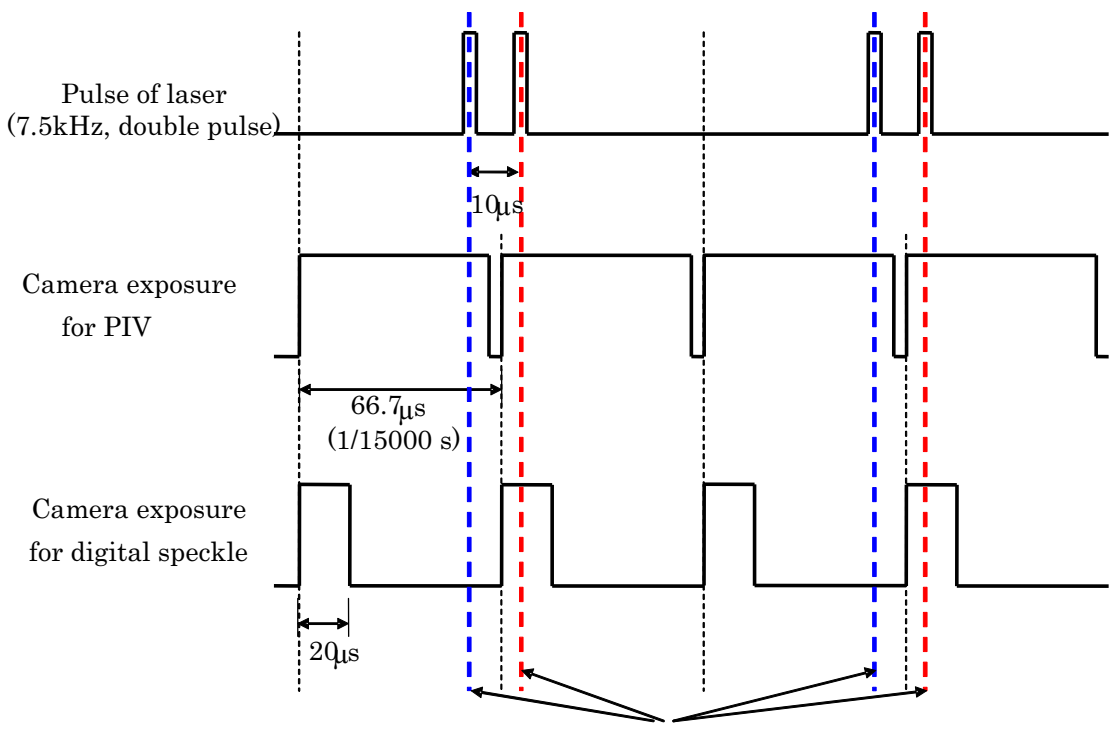

Fig. 4. Time table for synchronization.

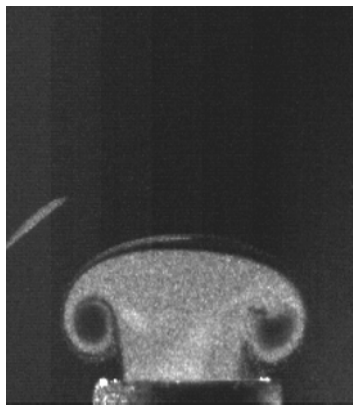

Fig. 5. Captured image for PIV at 25/15,000 second after opening nozzle.

5. Results and Discussion

The CO_2 flow from the elliptic nozzle has been examined using the digital speckle system and the PIV concurrently. Initially the oil particles have been suspended in the CO_2 at the nozzle with the

relative air pressure of 2 bars in the tube. After the first pulse signal of the synchronizer, the solenoid valve has been opened and three high-speed cameras have started capturing the images. The high-speed camera for the PIV has captured a pair of images as shown in Fig. 5 at every 2/15,000 second to analyze displacements of the seeding particles using the two-frame cross-correlation method. The maximum limitation of the measured velocity depends on the interrogation area and the searching window for the cross-correlation of the PIV. Since the length of the searching window is 32 pixels in this study, the maximum limitation of the measured velocity can be calculated to be 200 m/s, which is enough to measure the maximum velocity (130 m/s) in this condition.

The other two high-speed cameras for the digital specklegram have captured images at every 1/15,000 second and the cross-correlation has been performed for the displacement of the speckles by comparing between the image with no flow and the image with the CO_2 flow as shown in Figs. 6 (a) and (b). The speckle size for the digital speckle tomography is about 140μm in this study. The dynamic range of the measured density depends on the speckle movement which can be varied by the distance between the test section and the viewing screen for this case. Thus, the searching area for the speckle displacement should be determined to capture the maximum speckle movement. If the maximum movement can be captured in the determined searching window, the other speckle movements can be included in the searching windows to calculate the deflection angle which is expressed by the integration of the density gradient in Eq. (1). The distance of the maximum speckle displacements in Fig. 6 (c) is 163μm in the actual size of the field in Figs. 6 (a) and (b) with the height of 41.4mm and the width of 41.4mm. Therefore, the two-dimensional velocity distributions and the three-dimensional density distributions can be reconstructed at every 2/15,000 second.

After the solenoid valve has been opened, the compressed CO_2 has been exhausted suddenly into the air. The measured maximum speed of the CO_2 flow was about 130m/sec with the Mach number of about 0.5. The acceleration of the CO_2 flow has been observed as time passes in Fig. 7. The maximum velocity of the CO_2 flow at 25/15,000 second after opening the valve was 44.8 m/sec, 89.0 m/sec at 27/15,000 second, 108.0 m/sec at 29/15,000 second, and 120.8 m/sec at 31/15,000 second as shown in Fig. 8 for the contours of the velocity magnitude.

Although minimum three projection angles are required to reconstruct asymmetric density fields, the accurate density distributions of the CO_2 flow could be computed by two projection angles in this study since a bi-cubic interpolation technique has been performed to increase the number of images from 256×256 to 1024×1024 for improvement of the resolution. The laser beam of the digital speckle tomography is deflected three-dimensionally before reaching at the screen because of three-dimensional density variation. Thus, the three-dimensional tomography with two projection angles in each plane and 60 planes has been used in this study to analyze the projected ray sums which have the three-dimensional information of the deflected laser beam. 150 projection data for each projection angle have been obtained for the cross-correlation method, then the three dimensional density distribution with 25×25×25 pixels have been reconstructed by a computer with Intel Pentium-4 3.0GHz processor and 1.0GByte memory. Although the nozzle shape is elliptical, the flow structure may become complicated by the generated vortices from the continuous size variation along the ellipse (Shao et al, 2007). Thus, the flow structure should be investigated carefully to avoid the optical error for the PIV and the digital speckle tomography. The reliability of the present method has already been confirmed using the numerical simulation in the previous studies (Ko et al., 2004; Ko et al., 2006).

Figure 9 shows areas of the acquired image, projection data, reconstructed field and position of the nozzle. The area of the projection data is larger than that of the reconstruction because the projected ray should include the square reconstructed field. The width of projection data (41.4mm) should be about 1.4 times of that of the reconstructed field (29.6mm) and two images are overlapped in Fig. 9. Figure 10 shows reconstructed four-dimensional density distributions with various times and heights. Since the density distribution has been reconstructed from 9.1mm above the nozzle to 18.1mm as shown in Fig. 10, the reconstructed field is also smaller than the acquiring image for the height in Fig. 9. The reconstruction for the density distributions has been carried out from 9.1mm to

18.1mm from the nozzle to be confirmed with the velocity distribution from 27/15,000 second to 33/15,000 second in Fig. 10. Although three-dimensional volume has been reconstructed with time, the results of the density distributions are shown at the surfaces of 9.1mm and 18.1mm above the nozzle in Fig. 10 because three-dimensional results for all heights cannot be included on the paper. Since the reference value is the air density, the density value has been normalized between 0 and 1 in this study. Thus, the pure air density of 1.2 kg/m^3 in this condition is 0 and the pure CO_2 of 1.8 kg/m^3 is 1 in Fig. 10.

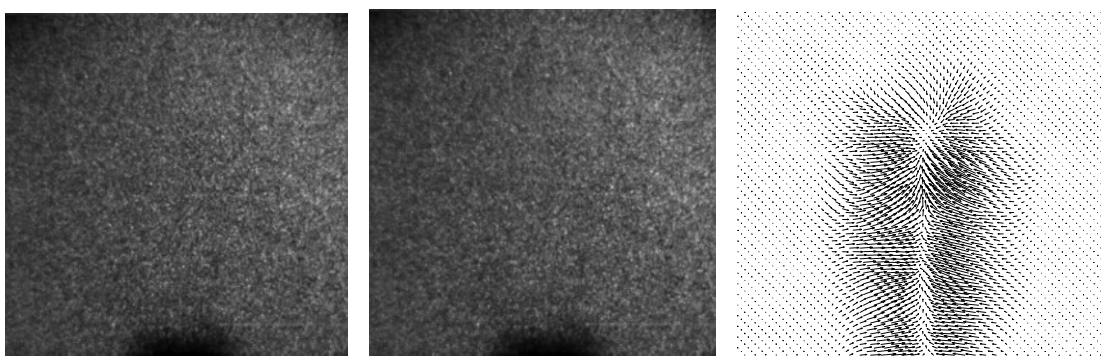

(a) No flow (b) CO_2 flow (c) Speckle displacements

Fig. 6. Captured images for digital speckle system at 27/15,000 second after opening nozzle.

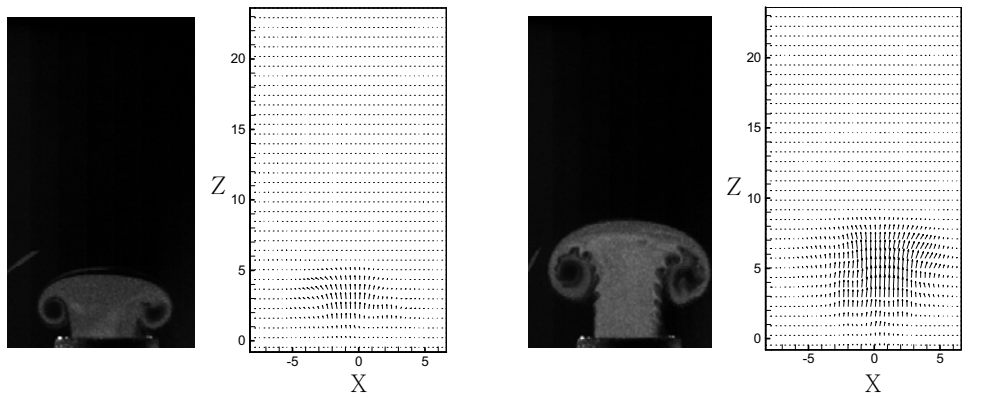

(a) 25/15,000 second (b) 27/15,000 second

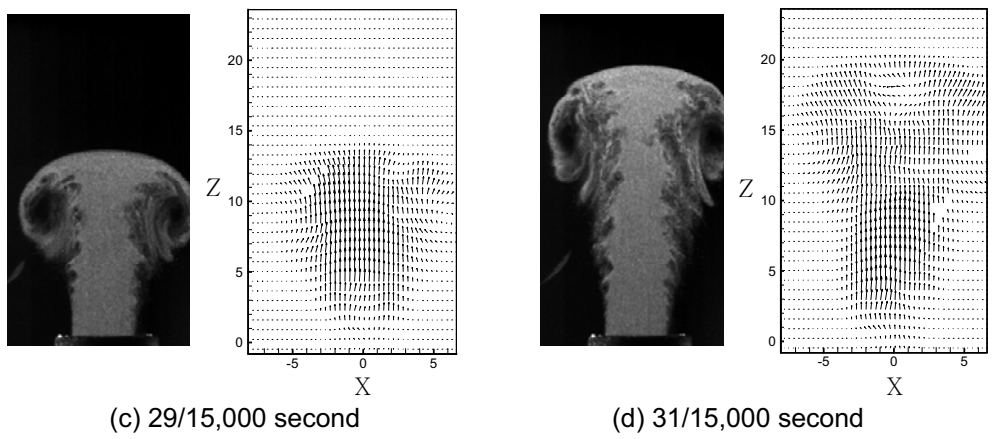

(c) 29/15,000 second (d) 31/15,000 second

Fig. 7. Measured PIV images and velocity distributions with time variation for high-speed CO_2 flow.

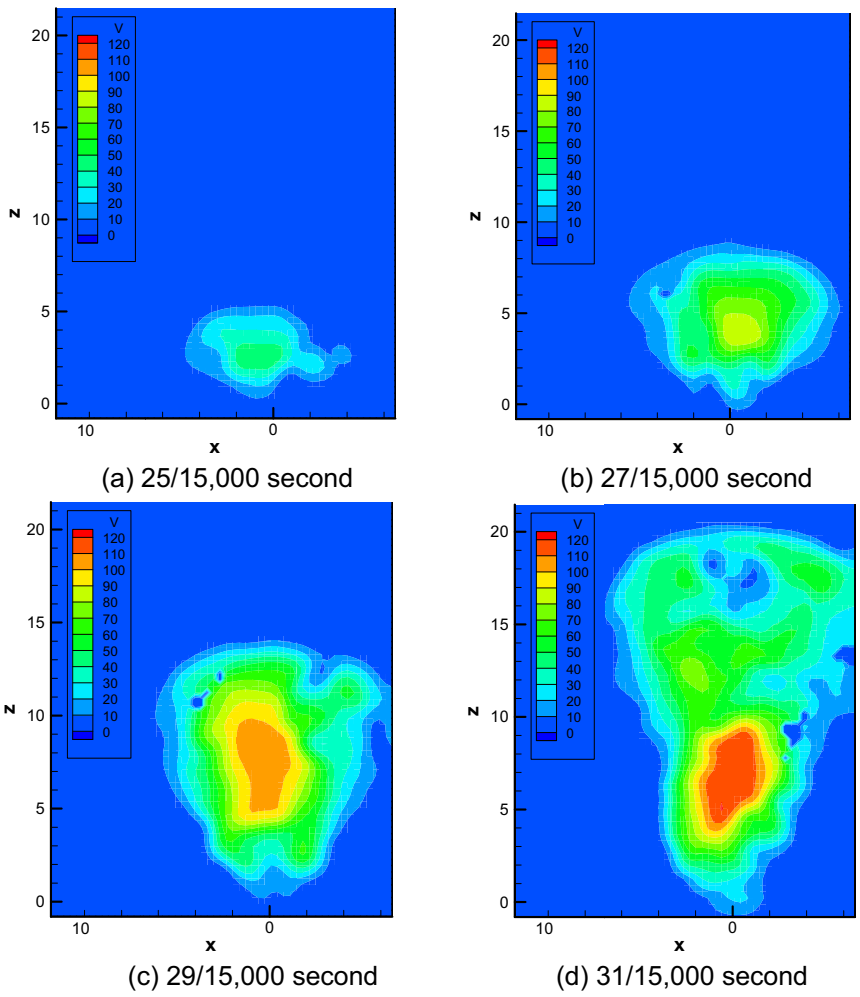

(a) 25/15,000 second (b) 27/15,000 second

(c) 29/15,000 second (d) 31/15,000 second

Fig. 8. Contours of velocity magnitude for high-speed CO_2 flow by PIV.

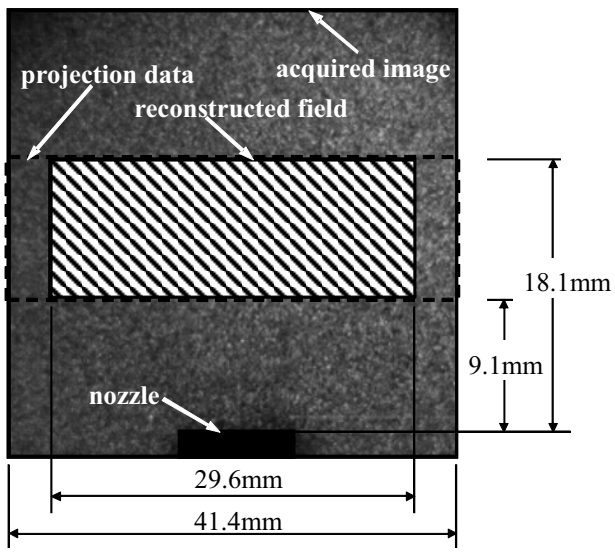

Fig. 9. Area of reconstructed field above nozzle.

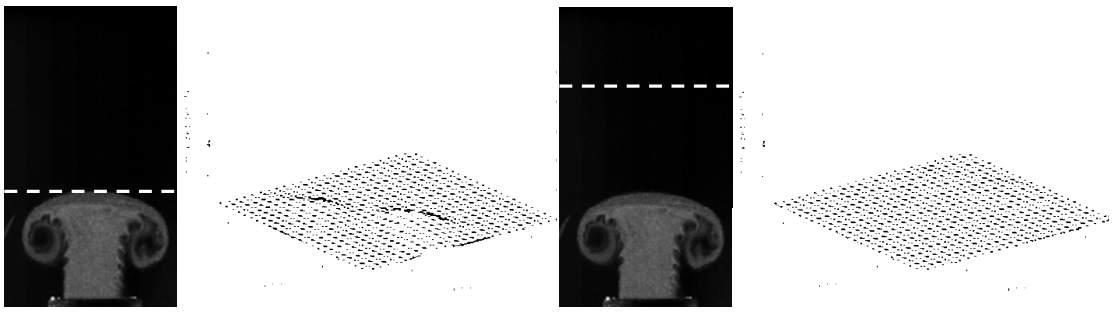

(a) 27/15,000 second at 9.1mm (b) 27/15,000 second at 18.1mm

(c) 29/15,000 second at 9.1mm (d) 29/15,000 second at 18.1mm

(e) 31/15,000 second at 9.1mm (f) 31/15,000 second at 18.1mm

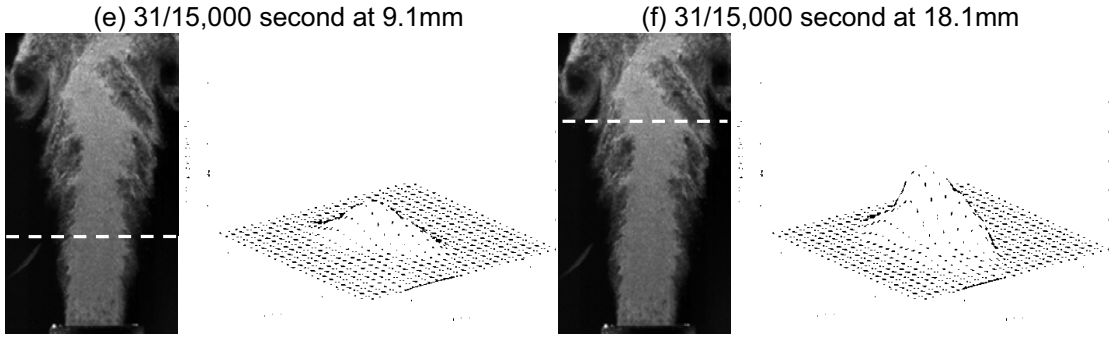

(g) 33/15,000 second at 9.1mm (h) 33/15,000 second at 18.1mm

Fig. 10. Reconstructed density distributions with height and time variation for high-speed CO_2 flow.

Some density variations which are supposed to be a head of the vortex ring have been observed at 27/15,000 second after opening the nozzle at 9.1mm above the nozzle while there is no change for 18.1mm above the nozzle. At 29/15,000 second, the big and wide elliptical density distribution which is considered to be a middle of the vortex ring at 9.1mm above the nozzle and little variation which can be the head of the ring has been shown at 18.1mm above the nozzle. The big elliptical density distribution has been observed at 18.1mm above the nozzle with 31/15,000 second while small elliptical density distribution has appeared at 9.1mm above the nozzle. At 33/15,000 second, the mid-sized elliptical density distributions have been shown at 18.1mm and 9.1mm above the nozzle, which is the steady-state density distribution after movement of the vortex ring. Same phenomena

have already been analyzed for the velocity distributions (Fig. 7). Therefore, the accuracies of the reconstruction can be confirmed by the concurrent measurement techniques using the PIV for the velocity distributions and the digital speckle system for the density distributions each other to analyze the fast and unsteady flows.

6. Conclusion

The combined system of the digital speckle tomography and the PIV has been proposed in this study. The three-dimensional density fields and two-dimensional velocity fields of the high-speed and starting CO_2 flow have been reconstructed concurrently at every 2/15000 second using three high-speed cameras. The vortex ring of the starting CO_2 flow has been observed and analyzed by the combined system. One of the essential conditions for the accuracy of the PIV is that the oil particles should follow perfectly to the CO_2 flow. Thus, the digital speckle tomography has been performed to reconstruct the density variations for comparing the time sequences of the velocity variations with those of the density variations for the starting CO_2 flow. The accuracy of the particle movement has been confirmed with the time sequences by the concurrent experiments of the PIV and the digital speckle tomography for the fast and unsteady CO_2 flow.

Acknowledgments

This work was performed at the University of Tokyo. This work was also partially supported by the Korea Research Foundation Grant funded by the Korean Government (MOEHRD) (KRF-2005-D00045 (I01474)).

References

Carlsson, T. E., Mattsson, R., Gren, P., Elfsberg, M. and Tegner, J., Combination of schlieren and pulsed TV holography in the study of a high-speed flame jet, Optics and Lasers in Engineering, 44 (2006), 535-554.

Erkan, N., Shinohara, K., Okamoto, K., Okamoto, T. and Fujii, T., Measurement of Two Overlapped Velocity Vector Fields in Microfluidic Devices Using Time-Resolved PIV, J. of Visualization, 11 (2008), 33-34.

Fomin, N. A., Speckle Photography for Fluid Mechanics Measurements (1998), Springer, Berlin.

Fujisawa, N., Funatani, S. and Watanabe, Y., Simultaneous Imaging Techniques for Temperature and Velocity Fields in Thermal Fluid Flows, J. of Visualization, 11 (2008), 247-256.

Gordon, R., A Tutorial on ART, IEEE Trans. Nuclear Sci. NS-21 (1974), 78-92.

Huang, C., Gregory, J. W. and Sullivan, J. P., A modified schlieren technique for micro flow visualization, Meas. Sci. Technol., 18 (2007), N32-N34.

Ko, H. S., Ikeda, K., Ishikawa, M., Okamoto, K. and Kim, Y. –J., 2Experimental Analysis of High-speed Helium Jet Flow Using Four-dimensional Digital Speckle Tomography, Exp. Fluids, 40 (2006), 442-451..

Ko, H. S., Ikeda, K. and Okamoto, K., Combination of Holographic Interferometry and Digital Speckle System for Measurement of Density Distributions, Meas. Sci. Technol., 13 (2002), 1974-1978.

Ko, H. S. and Kihm, K. D., An Extended Algebraic Reconstruction Technique (ART) for Density-Gradient Projections: Laser Speckle Photographic Tomography, Exp. Fluids, 27 (1999), 542-550.

Ko, H. S., Okamoto, K. and Madarame, H., Reconstruction of Transient Three-dimensional Density Distributions Using Digital Speckle Tomography, Meas. Sci. Technol., 12 (2001), 1219-1226.

Ko, H. S., Park, K. -H and Kim, Y. –J., Analysis of Density Distribution for Unsteady Butane Flow Using Three-dimensional Digital Speckle Tomography, KSME Int. J., 18 (2004), 1213-1221.

Mattsson, R., Kupiainen, M., Gren, P., Wåhlin, A., Carlsson, T. E. and Fureby, C., Pulsed TV holography and schlieren studies, and large eddy simulations of a turbulent jet diffusion flame, Combustion and Flame, 139 (2004), 1-15.

Partington, J. R., Physico-Chemical Optics IV (1953), Longmans Green, London.

Raffel, M., Willert, C. E. and Kompenhans, J., Particle Image Velocimetry (1998), Springer, Berlin.

Shao, C. P., Wang, J. M. and Wei, Q. D., Visualization Study on Suppression of Vortex Shedding from a Cylinder, J. of Visualization, 10 (2007), 57-64.

Trinite, M., Lecordier, B. and Lecerf, A., Simultaneous Development of Time Resolved Laser Tomography and PIV for Flames Propagation Studies, J. of Visualization, 2 (2000), 245-256.

Verhoeven, D., Limited-data computed tomography algorithms for the physical sciences, Applied Optics, 32 (1993), 3736-3754.

Vest, C. M., Holographic Interferometry (1979), Wiley, New York.

Wong, T. and Agrawal, A. K., Quantitative measurements in an unsteady flame using high-speed rainbow schlieren deflectometry, Meas. Sci. Technol., 17 (2006), 1503-1510.

Author Profile

Yong-Jae Kim: He received his B.S., M.S. and Ph.D. degrees in School of Mechanical Engineering from Sungkyunkwan University, Suwon, Korea, in 2001, 2003 and 2009, respectively. He works in Intelligent System Research Center, Sungkyunkwan University, Korea, as a postdoctoral research associate. His research interests are flow visualization (tomography and PIV) and electrohydrodynamics jet (EHD jet).

Koji Okamoto: He received his M.Sc .(Eng) in Nuclear Engineering in 1985 from University of Tokyo. He also received his Ph.D. in Nuclear Engineering in 1992 from University of Tokyo. He worked in Department of Nuclear Engineering, Texas A & M University as a visiting associate professor in 1994. He works in Department of Human and Engineered Environmental Studies, University of Tokyo as a professor since 1993. His research interests are Quantitative Visualization, PIV, Holographic PIV Flow Induced Vibration and Thermal-hydraulics in Nuclear Power Plant.

Han Seo Ko: He received his M.S. and Ph.D..degrees in Mechanical Engineering in 1994 and 1998, respectively from Texas A&M University. After obtaining Ph.D., he worked as a research associate at Nuclear Engineering Research Laboratory, University of Tokyo. He also worked in Department of Mechanical Engineering, Johns Hopkins University as a visiting associate professor in 2007~2008. He works in School of Mechanical Engineering, Sungkyunkwan University, Korea, as an associate professor since 2001. His current research interests are Flow Visualization, Microfluidics, Optical Tomography and Control of Micro-droplet Ejection.